Am J Cancer Res 2021;11(7):3698-3710
www.ajcr.us /ISSN:2156-6976/ajcr0134316

Original Article

Targeting mitotic exit in solid tumors

Christine Greil[1], Julia Felthaus[1], Marie Follo[1], Gabriele Ihorst[2], Daniel Ewerth[1], Julia Schüler[3], Dominik Schnerch[1], Justus Duyster[1], Monika Engelhardt[1], Ralph Wäsch[1]

[1]Department of Hematology, Oncology and Stem Cell Transplantation, Medical Center - University of Freiburg, Faculty of Medicine, University of Freiburg, Freiburg, Germany; [2]Clinical Trials Unit, University of Freiburg, Faculty of Medicine, University of Freiburg, Germany; [3]Charles River Discovery Research Services Germany GmbH, Freiburg, Germany

Received April 15, 2021; Accepted June 12, 2021; Epub July 15, 2021; Published July 30, 2021

Abstract: Targeting mitosis by taxanes is one of the most common chemotherapeutic approaches in various malignant solid tumors, but cancer cells may survive antimitotic treatment with attainable *in vivo* concentrations due to mitotic slippage with a residual activity of the ubiquitin ligase anaphase-promoting complex (APC/C) and a continuous slow ubiquitin-proteasome-dependent cyclin B-degradation leading to mitotic exit. Therefore, blocking cyclin B-proteolysis via additional proteasome (PI) or APC/C-inhibition may have the potential to enhance tumor cell eradication by inducing a more robust mitotic block and mitotic cell death. Here, we analyzed this approach in different cell lines and more physiological patient-derived xenografts (PDX) from lung and breast cancer. The sequential combination of paclitaxel with the PI bortezomib enhanced cell death, but in contrast to the hypothesis during interphase and not in mitosis in both lung and breast cancer. APC/C-inhibition alone or in sequential combination with paclitaxel led to strong mitotic cell death in lung cancer. But in breast cancer, with high expression of the anti-apoptotic regulator Mcl-1, cell death in interphase was induced. Here, combined APC/C- and Mcl-1-inhibition with or without paclitaxel was highly lethal but still resulted in interphase cell death. Taken together, the combination of antimitotic agents with a clinically approved PI or inhibitors of the APC/C and Mcl-1 is a promising approach to improve treatment response in different solid tumors, even though they act entity-dependent at different cell cycle phases.

Keywords: Antimitotic therapy, APC/C, proteasome inhibition, cyclin B, Mcl-1

Introduction

Targeting mitosis with spindle poisons like taxanes and vinca alkaloids that induce mitotic arrest by disturbing the microtubule assembly is a common approach to treat various malignancies [1]. Although several studies with cancer cell lines could prove a sustained mitotic arrest after treatment with high-dosed paclitaxel [2], it was shown in breast cancer that *in vivo* attainable concentrations do not induce a mitotic arrest, but multipolar spindles, resulting in chromosome missegregation and increased postmitotic cell death [3, 4]. Mechanistically, in adequate dosage taxanes may prevent the spindle assembly checkpoint (SAC) from being satisfied by interfering with microtubule kinetics [5] and trigger a continuous inhibition of the anaphase-promoting complex (APC/C). The APC/C is an E3-ubiquitin ligase that, after activation by the regulatory subunit Cdc20, leads to the proteasomal degradation of critical cell cycle regulators like the anaphase-inhibitor securin and the mitotic cyclin B to initiate chromosome separation and mitotic exit, respectively [6-11]. An incorrect kinetochore-microtubule attachment leads to formation of the mitotic checkpoint complex, that inhibits APC/C-activation by sequestration of Cdc20. Continuous APC/C-inhibition and consequently persistent high levels of cyclin B arrest cells in mitosis in order to provide additional time to resolve the spindle damage. In this way, spindle poisons can induce a cell cycle delay that can either trigger apoptosis during mitotic arrest mediated by mitochondrial outer membrane permeabilization and subsequent caspase activation in a p53-independent manner [12] or result in mitotic exit despite incomplete cell division and proliferation of cells with a highly aberrant genome [13].

Table 1. Overview of the examined Non-small cell lung cancer (NSCLC) and breast cancer cell lines and patient-derived xenografts (PDX)

		Entity	
Cell line	A549	NSCLC	Adenocarcinoma
	H838		Adenocarcinoma
	H520		Squamous cell carcinoma
	H460		Large cell carcinoma
	JIMT-1	Breast cancer	Triple negative
	MDA MB231		Triple negative
	MDA MB468		Triple negative
	T47D		Hormone receptor-positive
PDX	LXFA-629L	NSCLC	Adenocarcinoma
	LXFE-66NL		Squamous cell carcinoma
	LXFL-1121L		Large cell carcinoma
	MAXF-0401	Breast cancer	Triple negative

Two mechanisms leading to survival of cancer cells after spindle damage and subsequent mitotic arrest and therefore to a diminished efficacy of antimitotic drugs have been proposed [14]:

First, mitotic slippage can occur due to residual APC/C-activity and continuous background cyclin B-degradation by the ubiquitin-proteasome system, and cells may survive due to premature mitotic exit [15-17]. Thus, blocking mitotic exit downstream of the SAC by inhibition of cyclin B proteolysis or the APC/C in cells treated with antimitotic drugs should lead to a more efficient eradication of those apoptosis-resistant, slippage-prone cells.

Second, efficient apoptosis following mitotic arrest may be prevented due to an imbalance between the Bcl-2 family members as key regulators of the mitochondrial apoptotic pathway [18]. Most important in this context is the Mcl-1 protein, which is overexpressed in several cancers [19-21].

Recently, the APC/C-inhibitors proTAME and apcin have been described [22]: Their combination (pT/A) increases the stability of APC/C-substrates and they synergistically prevent mitotic exit and induce apoptosis in tumor cells. APC/C-inhibitors have not been implemented in clinical trials yet, but preclinical data indicate a promising therapeutic approach, as proTAME increased mitotic arrest and apoptosis in paclitaxel-treated cell lines of different solid tumors [23-26]. Similarly, a number of small molecules inhibiting anti-apoptotic proteins like Mcl-1 have shown promising clinical activity to re-enable apoptosis in different malignancies [23, 27, 28].

Here, we examined the additional prevention of cyclin B-degradation by either inhibition of the proteasome or the APC/C in lung and breast cancer cells both considered responsible to treatment with taxanes [29].

Material and methods

Cell culture

All cell lines (**Table 1**) were characterized by DSMZ in 2020 (German Collection of Microorganisms and Cell Cultures GmbH, Braunschweig, Germany). The patient-derived xenografts (PDX, **Table 1**) and the respective whole exome sequencing data were provided by Charles River Discovery Research Services Germany GmbH, Freiburg, Germany. All cells were tested for mycoplasma. A549, H838, H520, H460 and the PDX were cultured in RPMI1640-medium with L-glutamine (Thermo Fisher Scientific, MA, USA), 10% fetal bovine serum (FBS; Biochrom, Berlin, Germany), 1% penicillin/streptomycin, 1 mM sodium pyruvate and 25 mM Hepes (all Thermo Fisher Scientific, MA, USA). MDA MB213, MDA MB468 and JIMT-1 were cultured in DMEM-medium with D-glucose, L-glutamine and pyruvate (Thermo Fisher Scientific, MA, USA), 10% FBS and 1% penicillin/streptomycin. T47D were cultured in 90% IMEM-medium with L-glutamine (Thermo Fisher Scientific, MA, USA), 10% FBS, 1% penicillin/streptomycin and 1 mM sodium pyruvate. Cell culture was performed under standard conditions (37°C, 5% CO_2 (10% for JIMT-1), 90% air humidity).

Drug administration

Cells were treated with paclitaxel (Sigma-Aldrich, MO, USA) diluted in the appropriate medium to 118 nM for high-dose treatment and G2/M-block, or for low-dose treatment to 5.9 nM for LXFA-629L and MAXF-0401, to 8.8 nM for LXFE-66NL and to 11.7 nM for LXFL-1121L for 24 h. After a wash step with medium, either bortezomib (Selleckchem, Munich, Germany) diluted in the appropriate medium to

2.5 nM for MAXF-0401, 10 nM for LXFA-629L and LXFE-66NL and 25 nM for LXFL-1121L, or the combination of the two drugs proTAME and apcin (pT/A; both BostonBiochem, MA, USA) [22] diluted in the appropriate medium to the published effective concentrations of 16 µM and 200 µM in all cell lines and PDX, were added for another 24 h. The doses of paclitaxel and bortezomib used in the cell lines are indicated in Figures S1 and S2. S63845 (APExBIO, TX, USA) [31] was diluted in the appropriate medium to 1.5 µM and was applied for 48 h simultaneously with paclitaxel.

Calculation of half maximal effective concentration (EC_{50}) and combination index (CI)

The EC_{50} and CI were determined using the Quest Graph™ EC_{50} Calculator [32] and the CompuSyn software [33]. The therapy effect was defined as reduction of cell viability assessed by acridine orange/propidium iodide-double stain (LUNA-FL™ dual fluorescence cell counter). Three different concentration levels for each substance and combination in a fixed ratio were analyzed.

Soft agar colony assays

A bottom layer with 0.8% NuSieve™GTG™ agarose (Lonza, Köln, Germany) in medium was prepared in 35 mm-culture dishes. One ml medium containing 50,000 cells after the appropriate treatment as described above and after a wash step to remove the substances was mixed with 1 ml 1.4% agarose in medium and plated as top layer, covered with medium, and incubated under standard cell culture conditions. The number of colonies was counted at day 21.

Live cell imaging

Cells were seeded on eight-well chambered coverslips (Ibidi, 80826) with 30-50,000 cells per well and incubated under standard cell culture conditions for 24 h. The SiR-DNA kit (Spirochrome, Stein am Rhein, Germany) was used for nucleus stain. Image acquisition was performed on an Olympus (Hamburg, Germany) IX-81 inverse microscope with climate chamber using a UPLSAPO × 20 objective (numerical aperture 0.75) and the ScanR Acquisition software (v.2.2.09). RFP-fluorescence was visualized using a CY5-filter set. Picture acquisition was repeated every 10 min under standard climate chamber conditions. Analysis was performed using the ScanR analysis software (v.1.2.0.6).

Flow cytometry

Cell cycle distribution was assessed by DNA staining with propidium iodide and DNA content was measured based on fluorescence intensity by flow cytometry. Cells were fixed in 70% ethanol at 4°C over night, washed in PBS, incubated in 50 µg/ml propidium iodide containing 0.1 mg/ml RNaseA and 0.1% TritonX (all Sigma-Aldrich, MO, USA) for 30 min at 37°C and analyzed on a BD LSRFortessa™ cell analyzer (Becton Dickinson GmbH, Heidelberg, Germany). A standard of 10,000 cells was analyzed per sample or data point. Software analysis of cell cycle distribution was performed with BD FACSDiva™ Software (Becton Dickinson GmbH, Heidelberg, Germany).

Lentivirus-based knockdown plasmids and transduction

For knockdown (kd) of Mcl-1 oligonucleotides containing the target sequence 5'-GGACTG-GCTAGTTAAACAAAG-3' (shRNA1) or 5'-GAAGG-AAGTATCGAATTTACA-3' (shRNA2), the complementary sequence, a loop and linker sequences were designed as previously described [34] and ligated into pLentiLox 3.7 (pLL). 293T cells (ACC635, DSMZ, Braunschweig, Germany) were transfected with the pLL-kd vector and packaging plasmids (pMDLg/pRRE, pRSV-Rev, pMD.G) and incubated for 10 h in the presence of calcium phosphate-precipitated plasmid DNA. Virus-containing supernatant was collected after 24 and 48 h. MAXF-0401 cells were incubated in 4 ml of virus containing supernatant supplemented with 2 ml of fresh normal medium and 5 µg/ml hexadimethrine bromide.

Mutational analysis (whole exome sequencing)

After DNA extraction, material was sequenced with 126 bp paired-end reads using the ILLUMINA HiSeq-2500 platform and the Agilent V5 50MB enrichment kit, with a coverage of >160X. Next, human reads were isolated using Xenome [35], aligned to the GRCh38 reference genome, and mutations were called using a workflow based on GATK (Genome Analysis Toolkit version 4) best practices. Using the variant effect predictor (VEP) [36], candidate mutations were annotated and filtered

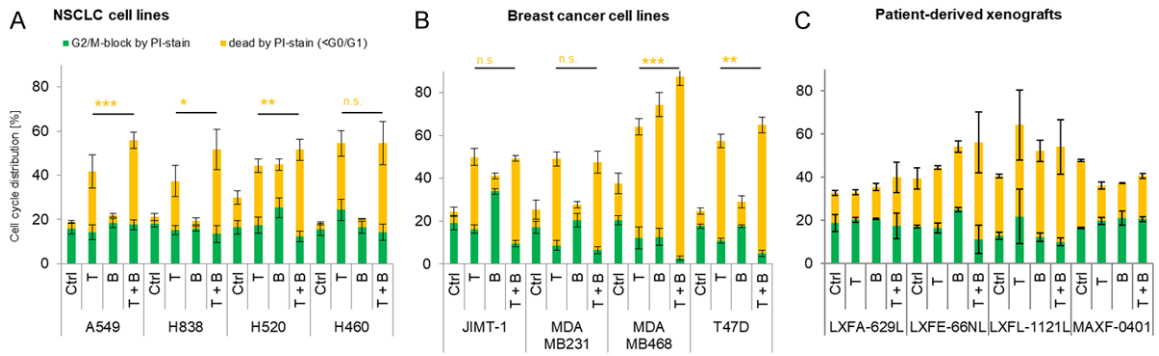

Figure 1. Combination of antimitotic treatment with proteasome inhibition leads to increased cell death in solid tumor cells. Response of (A) NSCLC (adeno- [A549, H838], squamous [H520], large cell carcinoma [H460]) and (B) breast cancer cell lines (triple negative [JIMT-1, MDA MB231, MDA MB468], hormone receptor-positive [T47D]) and (C) different PDX (NSCLC adenocarcinoma [LXFA-629L], squamous cell carcinoma [LXFE-66NL], large cell carcinoma [LXFL-1121L] and breast cancer [MAXF-0401]) to antimitotic therapy (T), proteasome inhibition (B) and the combination (T + B) was assessed by flow cytometry after propidium iodide-stain, the percentage of cells in G2/M-phase (green bars) and apoptotic cells (yellow bars) are depicted as compared to control; n=3 for cell lines, n=2 for PDX. Abbreviations: NSCLC = Non-small cell lung cancer; PDX = patient-derived xenograft; ctrl = untreated control; T = paclitaxel; B = bortezomib; ***P<0.001; **P<0.01; *P<0.05; n.s. = not significant.

considering only variants with moderate or high protein impact and those being rare in healthy populations (<1% in gnomAD) [37].

Western blot and antibodies

Cells were lysed using RIPA buffer (40 mM Tris Base, 150 mM NaCl, 1% NP-40, 0.5% Sodiumdeoxylat, 0.1% SDS, 1 mM EDTA) and freshly added to a complete protease- (Roche, Basel, Switzerland) and phosphatase-inhibitor cocktail set (Calbiochem Merck, Darmstadt, Germany). 50-100 mg protein was separated on 10% SDS-PAGE. Immunoblotting was performed with ImmobilonP membranes (Millipore, Billerica, CA, USA). Antibody incubation was performed in 5% skim milk powder in PBS. After each step, membranes were washed in PBS/0.1% Tween (Sigma-Aldrich). Antibodies used were anti-Bub1 (Bethyl Laboratories, TX, USA), anti-BubR1, anti-Mcl-1 (both Becton Dickinson GmbH, Heidelberg, Germany), anti-Mad2, anti-Cyclin B1 (both Santa Cruz Biotechnology, Heidelberg, Germany), anti-Cdc20, anti-Cdh1 (both Abcam Cambridge, UK), anti-cGAS, anti-phospho-Histone 3 (both Cell Signaling Technology, Frankfurt, Germany) and anti-Actin (Sigma-Aldrich, MO, USA). Horseradish-peroxidase-conjugated secondary antibodies used were anti-rabbit (GE Healthcare, Pittsburgh, PA, USA) and anti-mouse (Dako Cytomation, Glostrup, Denmark).

Statistics

Biological replicates were analyzed for all experiments. A two-sided Student's t-test was used for statistical analyses. Mean and standard deviation were plotted as indicated. *P*-values were defined as described in the figure legends.

Results

Proteasome inhibition in paclitaxel-treated solid cancer cells increases cell death in interphase

We evaluated the effect of paclitaxel in combination with the proteasome inhibitor (PI) bortezomib in various cell lines from non-small cell lung (NSCLC) and breast cancer (**Figure 1A**, **1B**; **Table 1**). In addition, we investigated *ex vivo* cultures of patient-derived xenografts (PDX), as these are closest to the biology of *in vivo* growing tumors [38, 39]. Cells from three NSCLC with the main different histologies and a triple-negative breast cancer PDX were used (**Table 1**).

A tumor type-specific concentration of the spindle poison paclitaxel and the PI bortezomib was chosen that can empirically be achieved *in vivo* [2], which just led to an increased G2/M-block (for paclitaxel) or an incipient increase of apoptotic rate (for bortezomib) in previously performed concentration series and

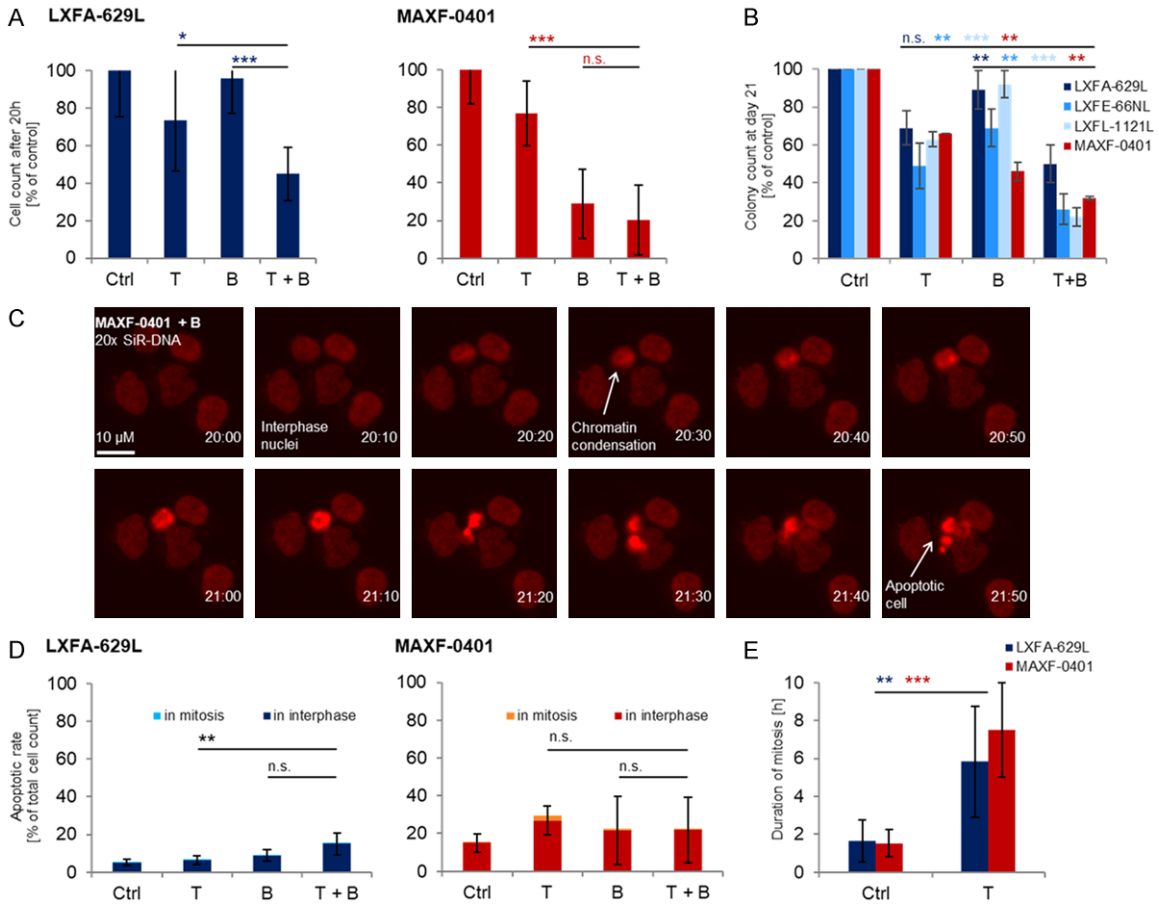

Figure 2. Proteasome inhibition in paclitaxel-pretreated solid cancer cells increases cell death in interphase. A. The total cell count was determined via live cell imaging of NSCLC adenocarcinoma ([LXFA-629L], blue bars) and breast cancer PDX ([MAXF-0401], red bars) 20 hours after DNA-stain (SiR) and antimitotic therapy (T), proteasome inhibition (B) and the combination (T + B); n=9. B. The long-term effect of the appropriate treatment on cell growth in three NSCLC (adenocarcinoma, squamous cell carcinoma [LXFE-66NL], large cell carcinoma [LXFL-1121L]) and the breast cancer PDX was examined with soft agar colony assays; n=3. C. The course of cell cycle leading to apoptosis was traced back on single cell level via live cell imaging, exemplary shown for breast cancer PDX after proteasome inhibition. The time point is indicated in h:min after addition of bortezomib. D. The rate of cells entering apoptosis during interphase vs. in mitosis, respectively, was quantified for NSCLC adenocarcinoma and breast cancer PDX; n=9. The *p*-values refer to the total apoptotic rate. E. Time from chromatin condensation to completion of telophase was determined for untreated NSCLC adenocarcinoma and breast cancer PDX and after antimitotic therapy, respectively; n=9. Abbreviations: PDX = patient-derived xenograft; NSCLC = Non-small cell lung cancer; ctrl = untreated control; T = paclitaxel; B = bortezomib; *P<0.05; **P<0.01; ***P<0.001; n.s. = not significant.

which lay in the range of the calculated half maximal effective concentration (EC_{50}; Figures S1 and S2).

As expected, the apoptotic rate of sequentially treated cells was significantly increased in most cancer cell lines after combination of paclitaxel with bortezomib when compared to paclitaxel alone (**Figure 1A**, **1B**). In the more physiological PDX, there was only a trend towards a higher toxicity of the combination when analyzing the sub-G1-fraction by flow cytometry (**Figure 1C**), but both cell counts shortly after exposure (**Figure 2A**) and long-term colony-forming capacity in soft-agar were significantly reduced, when comparing the effect of the single substances with the combination treatment (**Figure 2B**). Live cell imaging revealed that apoptosis was mainly initiated during interphase and not in mitosis in both PDX after *in vivo* attainable concentrations of paclitaxel, bortezomib and the combination of both substances (**Figure 2C**, **2D**). The total apoptotic rate was increased by additional

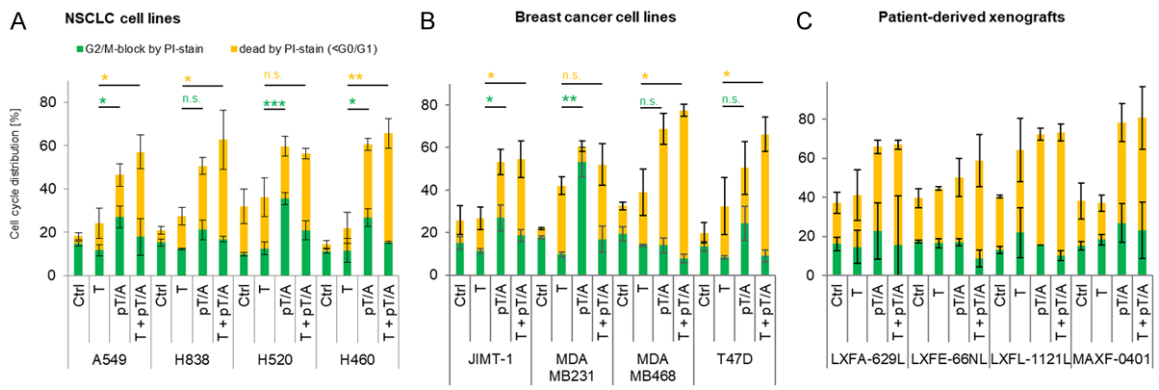

Figure 3. Combination of antimitotic treatment with APC/C-inhibition leads to increased cell death in solid tumor cells. Response of (A) NSCLC (adeno- [A549, H838], squamous [H520], large cell carcinoma [H460]) and (B) breast cancer cell lines (triple negative [JIMT-1, MDA MB231, MDA MB468], hormone receptor-positive [T47D]) and (C) different PDX (NSCLC adenocarcinoma [LXFA-629L], squamous cell carcinoma [LXFE-66NL], large cell carcinoma [LXFL-1121L] and breast cancer [MAXF-0401]) to antimitotic therapy (T), direct APC/C-inhibition (pT/A) and the combination (T + pT/A) was assessed by flow cytometry after propidium iodide-stain, the percentage of cells in G2/M-phase (green bars) and apoptotic cells (yellow bars) are depicted as compared to control; n=3 for cell lines, n=2 for PDX. Abbreviations: PDX = patient-derived xenograft; NSCLC = Non-small cell lung cancer; ctrl = untreated control; T = paclitaxel; pT/A = proTAME/apcin; ***P<0.001; **P<0.01; *P<0.05; n.s. = not significant.

bortezomib after paclitaxel treatment in NSCLC adenocarcinoma, but not in breast cancer PDX (**Figure 2D**). In accordance with the expected effect of spindle poisons, mitosis was significantly prolonged after treatment with paclitaxel in comparison to the untreated control in both PDX (**Figure 2E**).

Additionally, the combination index (CI) of paclitaxel and bortezomib was determined for these PDX: It was lower than one in NSCLC adenocarcinoma (CI=0.359), confirming a synergistic effect of the two substances (**Figure 2A**, **2B**), but greater than one in breast cancer PDX (CI=2.579) arguing against synergism, since bortezomib was already highly efficient on its own in this PDX (**Figure 2A**, **2B**).

APC/C-inhibition alone and in paclitaxel-pretreated cells increases cell death in mitosis in lung cancer and in interphase in breast cancer

Next, we evaluated the effect of paclitaxel in combination with the APC/C-inhibitors proTAME and apcin (pT/A) dosed in accordance with previous published *in vitro* data [22, 40]. Cell cycle distribution of the same set of different NSCLC and breast cancer cell lines and PDX was analyzed after monotherapy with paclitaxel, with pT/A and after combination treatment of paclitaxel with sequentially added pT/A, respectively (**Figure 3A-C**). We observed an enhanced G2/M-arrest after pT/A as compared to *in vivo* attainable paclitaxel concentrations in nearly all cell lines (**Figure 3A**, **3B**). The combination of both substances led to a lower G2/M-, but increased apoptotic rate, suggesting a higher incidence of apoptosis in mitosis (**Figure 3A**, **3B**). There was a clear trend for increased cell deaths after treatment with pT/A and paclitaxel as compared to the spindle poison alone in the four PDX (**Figure 3C**). In the short-term analysis via live cell imaging, cell counts were significantly reduced in lung and breast cancer PDX with this combination (**Figure 4A**). However, the long-term colony-forming capacity was only reduced in lung but not in breast cancer PDX (**Figure 4B**). Interestingly, in live cell imaging after APC/C-inhibition alone and in combination with paclitaxel, we observed that lung cancer cells mainly died in mitosis (**Figure 4C**, **4D**), but the majority of breast cancer cells died during interphase (**Figure 4D**). In both PDX, the total apoptotic rate was significantly increased by additional APC/C-inhibition after antimitotic treatment and already after APC/C-inhibition with pT/A alone (**Figure 4D**).

The CI for paclitaxel and pT/A was lower than one in NSCLC adenocarcinoma (CI=0.566), confirming the presumed synergistic effect of the two substances in this entity, but greater than one in breast cancer PDX (CI=1.084), arguing against synergism.

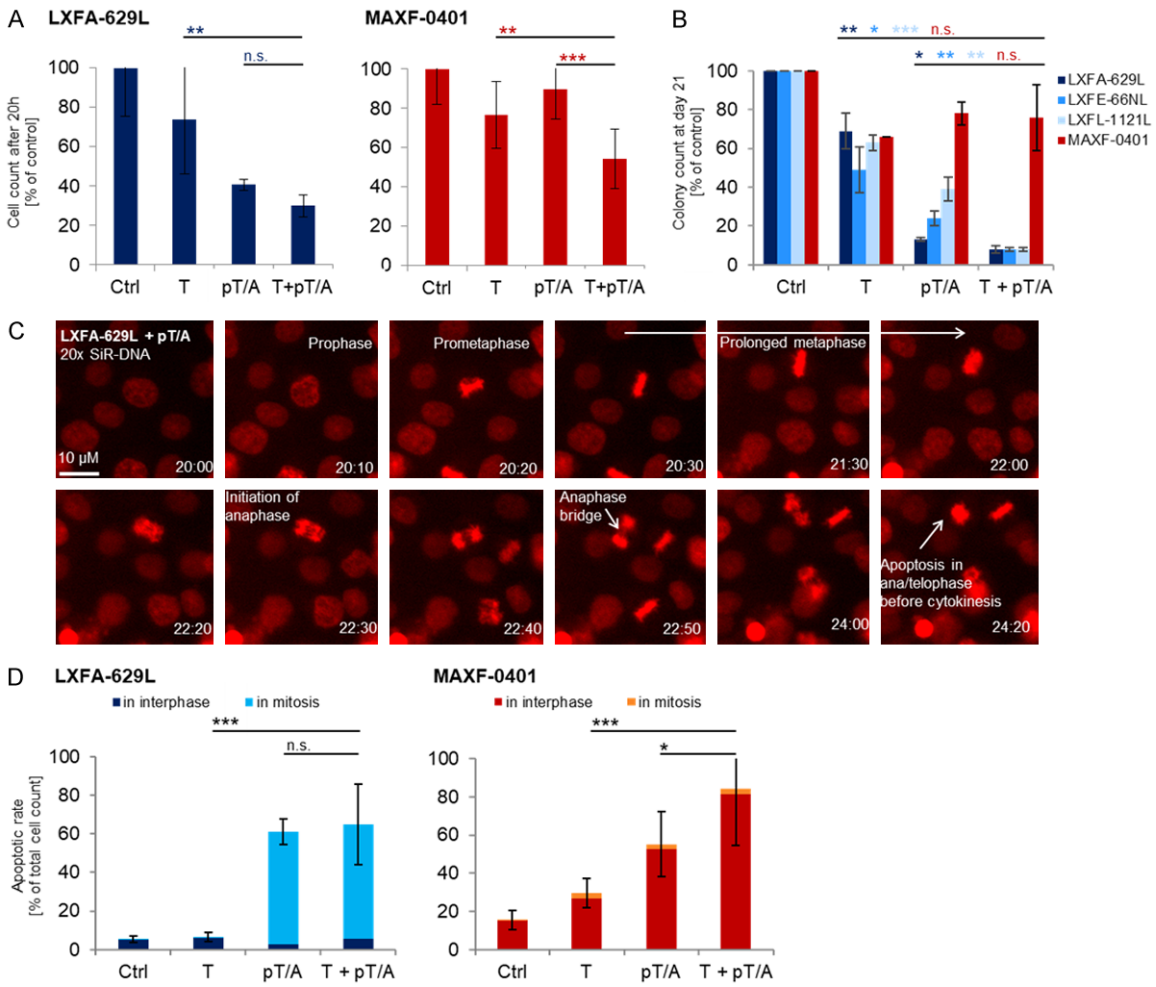

Figure 4. APC/C-inhibition alone and in paclitaxel-pretreated cells increases cell death in mitosis in lung cancer and in interphase in breast cancer. A. The total cell count was determined via live cell imaging of NSCLC adenocarcinoma ([LXFA-629L], blue bars) and breast cancer PDX ([MAXF-0401], red bars) 20 hours after DNA-stain (SiR) and antimitotic therapy (T), APC/C-inhibition (pT/A) and the combination (T + pT/A); n=9. B. The long-term effect of the appropriate treatment on cell growth in three NSCLC (adenocarcinoma, squamous cell carcinoma [LXFE-66NL], large cell carcinoma [LXFL-1121L]) and the breast cancer PDX was examined with soft agar colony assays; n=3. C. The course of cell cycle leading to apoptosis was traced back on single cell level via live cell imaging, exemplary shown for NSCLC adenocarcinoma PDX after APC/C-inhibition. The time point is indicated in h:min after addition of pT/A. D. The rate of cells entering apoptosis during interphase vs. in mitosis, respectively, was quantified for NSCLC adenocarcinoma and breast cancer PDX; n=9. The *p*-values refer to the total apoptotic rate. Abbreviations: PDX = patient-derived xenograft; NSCLC = Non-small cell lung cancer; ctrl = untreated control; T = paclitaxel; pT/A = proTAME/apcin; *P<0.05; **P<0.01; ***P<0.001; n.s. = not significant.

The anti-apoptotic protein Mcl-1 is overexpressed in the breast cancer PDX and its inhibition is highly toxic but still induces cell death in interphase and not in mitosis

As whole exome sequencing data of the four PDX (**Table 2**) did not provide an obvious explanation for the different responses to APC/C-inhibition of the distinct tumor entities, the expression of mitotic and anti-apoptotic regulators was examined at protein level in the untreated PDX (**Figure 5A**). Most strikingly, and consistent with known properties of this entity [41], the anti-apoptotic protein Mcl-1 was substantially upregulated in the triple negative breast cancer PDX (**Figure 5A**), suggesting that the efficacy of antimitotic treatment using paclitaxel and pT/A in these cells may be influenced by Mcl-1-overexpression. Mcl-1 levels of the different PDX blocked in G2/M-phase after high-dosed paclitaxel were comparable to the untreated controls (Figure S3A) and remained

Table 2. Detected aberrations in whole exome sequenzing of the NSCLC squamous cell [LXFE-66NL], large cell [LXFL-1121], adenocarcinoma [LXFA-629L] and breast cancer [MAXF-0401] patient-derived xenografts

Gene	LXFA-629L	LXFE-66NL	LXFL-1121L	MAXF-0401
APC	nonsense	wild type	nonsense	missense
BRCA1	nonsense	wild type	wild type	frameshift
BRCA2	nonsense	frameshift	wild type	wild type
CDKN2A	*low coverage*	missense	wild type	*low coverage*
CDKN2B	*low coverage*	wild type	wild type	*low coverage*
CTNNB1	missense	wild type	wild type	wild type
EGFR	nonsense	wild type	wild type	wild type
ERBB2	missense	wild type	wild type	wild type
ERBB3	frameshift	wild type	wild type	wild type
FGFR3	wild type	wild type	wild type	*low coverage*
KIT	frameshift	wild type	wild type	wild type
KRAS	wild type	wild type	wild type	wild type
LRP1B	nonsense	wild type	missense	wild type
MET	frameshift	wild type	wild type	wild type
MLH1	frameshift	wild type	wild type	wild type
MSH3	missense	wild type	wild type	wild type
MYC	wild type	wild type	wild type	wild type
NOTCH1	missense	wild type	*low coverage*	*low coverage*
PIK3CA	nonsense	wild type	wild type	wild type
PIK3CB	nonsense	wild type	wild type	wild type
PIK3R1	wild type	wild type	wild type	wild type
PTEN	wild type	wild type	wild type	wild type
STK11	*low coverage*	wild type	wild type	*low coverage*
TP53	missense	missense	missense	missense
sVEGFA	wild type	wild type	wild type	wild type

high after treatment with pT/A in the breast cancer PDX (Figure S3B). APC/C-inhibition with or without paclitaxel, but not paclitaxel alone at *in vivo* attainable concentrations, led to increased pH3-levels, indicating a more pronounced block in metaphase, and cyclin B-levels remained largely unchanged independent of the respective treatment in all PDX as expected in whole cell extract (Figure S3B).

We repeated colony assays with the breast cancer PDX after treatment with paclitaxel and/or pT/A in combination with the Mcl-1-inhibitor S63845 [31]. Indeed, colony formation was significantly reduced after addition of S63845 to both the APC/C-inhibitor alone and the combination of paclitaxel with pT/A (**Figure 5B**). The supplementary CI-calculation indicated a synergistic effect of combined APC/C- and Mcl-1-inhibition with a value lower than one (CI=0.061). To confirm that these results were specific to Mcl-1-inhibition, we repeated the experiments using two different shRNA against Mcl-1 with different knockdown (kd) efficacy (**Figure 5C**) and observed a synergism of Mcl-1-kd with APC/C-inhibition and antimitotic treatment in a dose-dependent manner, with Mcl-1-kd being much more toxic on its own than the less specific inhibitor (**Figure 5D**). However, live cell imaging of the breast cancer PDX after additional Mcl-1-inhibition revealed that the leading cause of toxicity was still apoptosis in interphase (**Figure 5E**, **5F**).

Discussion

Taxanes play an important role in the treatment of breast, ovarian and lung cancer since the 1990s [4], but the antitumor effect and thus the clinical efficacy of these spindle poisons are highly variable [14]. The mechanism leading to cell death is still not fully under-

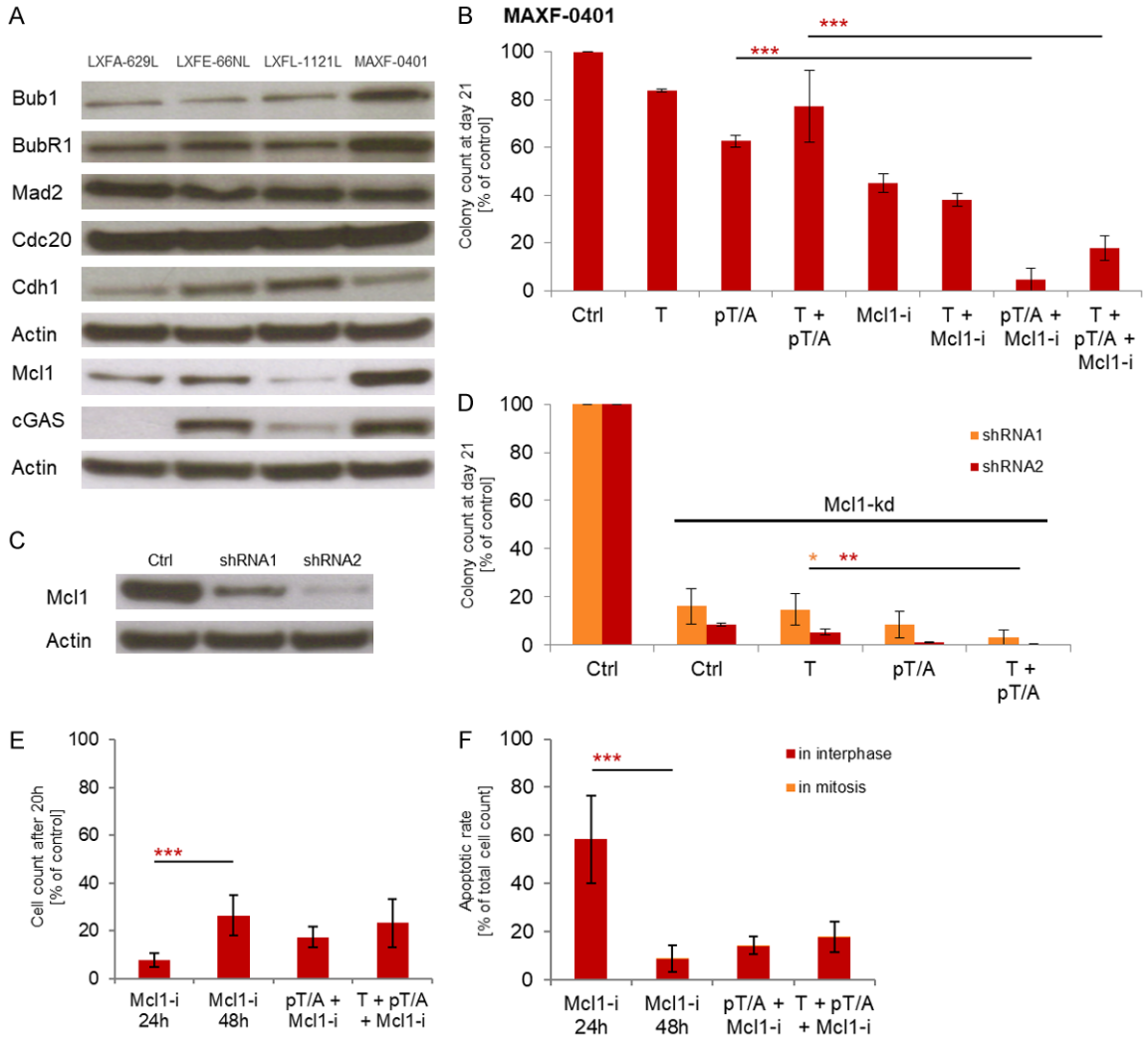

Figure 5. The anti-apoptotic protein Mcl-1 is overexpressed in the breast cancer PDX and its inhibition is highly toxic but still induces cell death in interphase and not in mitosis. (A) Expression of mitotic and antiapoptotic regulators in untreated NSCLC squamous cell carcinoma [LXFE-66NL], adenocarcinoma [LXFA-629L], large cell carcinoma [LXFL-1121L] and breast cancer PDX [MAXF-0401] was analyzed by western blot. Blots for Bub1/BubR1, Mad2/Cdc20/Cdh1 and Mcl-1/cGAS were cropped from different parts of the same gel. (B) In addition to antimitotic therapy (T) and APC/C-inhibition (pT/A), the breast cancer PDX was treated with the Mcl-1-inhibitor S63845 (Mcl1-i) and soft agar colony assays were performed to determine long-lasting antitumor effects; n=3. (C) After Mcl-1-knockdown with two different shRNA, (D) soft agar colony assays were performed with the breast cancer PDX to analyze the impact on cell growth of the spindle poison (T), the APC/C-inhibitor (pT/A) and the combination (T + pT/A); each n=2. Live cell imaging of the breast cancer PDX was performed after DNA-stain (SiR), (E) the total cell counts and (F) the rate of cells entering apoptosis during interphase vs. in mitosis, respectively, was quantified after the appropriate treatment; n=9. Abbreviations: PDX = patient-derived xenograft; NSCLC = Non-small cell lung cancer; ctrl = untreated control; T = paclitaxel; pT/A = proTAME/apcin; Mcl1-i = Mcl-1-inhibitor; Mcl1-kd = Mcl-1-knockdown; *P<0.05; **P<0.01; ***P<0.001.

stood. Induction of mitotic delay is supposed to play a pivotal role [42], and several *in vitro* studies with cancer cell lines could prove a sustained mitotic arrest after treatment with high-dosed paclitaxel [2]. However, it was shown that lower therapeutically relevant concentrations do not induce a mitotic arrest, but multipolar spindles, resulting in chromosome missegregation and increased cell death in interphase following a perturbed mitosis [3, 43]. Paclitaxel is known to accumulate intracellularly, depending on the cell type and concentration: in breast cancer cell culture, treatment with 5-10 nM paclitaxel resulted in intracellu-

lar concentrations of 1-9 μM; similar intratumoral concentrations were measured in breast cancer tissue samples 20 h after intravenous administration of an usual dose of 175 mg/m^2 [3]. According to these results, we chose clinically relevant low concentrations for our analyses, similarly low as the calculated EC_{50}. We observed a significantly prolonged mitosis after treatment with paclitaxel at these concentrations in comparison to control in live cell imaging of the examined PDX, but the rate of apoptosis in mitosis was not increased, indicating a delayed but successful completion of mitosis. Thus, mitotic delay by SAC-activation and APC/C-inhibition and mitotic slippage could play a role even at these low, *in vivo* attainable concentrations. It has recently been shown that preventing mitotic slippage by downregulation of the APC/C-co-activator Cdc20 may increase the sensitivity of cancer cells to spindle poisons [17, 42] and high Cdc20-expression levels have been reported in human cancers, often associated with an unfavorable prognosis [44, 45]. Additionally, a combination treatment may enable further dose reductions and could help to avoid typical side effects of taxanes, mainly peripheral neuropathy [29]. In accordance with this assumed synergistic inhibition of mitotic exit, and as already described in ovarian cancer [24], we observed the most impressive effect on tumor growth in three different NSCLC PDX after addition of the APC/C-inhibitors pT/A to paclitaxel-pretreatment and already after pT/A alone [40]. Here, we proved an increased rate of apoptosis after prolonged meta/anaphase by pT/A-addition, whereas in the examined breast cancer PDX, APC/C-inhibition was less efficient and the majority of cells entered apoptosis during interphase. The colony assays confirmed the expected durable treatment response due to apoptosis in mitosis in the NSCLC PDX. In contrast, we observed long-term recovery in the breast cancer PDX with only slightly reduced colony formation capacity despite the increased apoptotic rate and thus reduced cell count shortly after exposition. A difference in short- vs. long-term survival of cells due to mitotic slippage has already been described [43]: it may prevent mitotic cell death caused by spindle poisons in the short-term course, but could increase long-term cytotoxicity due to accumulated genomic instability after incorrect chromosome segregation. In line with this hypothesis, we observed increased toxicity shortly after APC/C-inhibition, but long-term survival was not reduced.

We assumed a persistent high level of the anti-apoptotic regulator Mcl-1 to be the underlying cause for the entity-specific observations as it is frequently overexpressed in breast cancer and may mediate resistance to conventional antitumor therapy [46]. Mcl-1-levels are regulated cell cycle-dependent with a peak in G2-phase and an APC/C-mediated decrease during mitosis [21]. This decline is supposed to promote apoptosis of cells arrested in mitosis and it has been shown that persistent high Mcl-1 levels inhibit apoptosis after antimitotic treatment [21, 47]. Indeed, in our breast cancer PDX, the most impressive reduction of cell growth was achieved with the combination of APC/C- and Mcl-1-inhibition by using selective Mcl-1-inhibitors as well as by Mcl-1-kd. However, contrary to prior observations in ovarian cancer [24], our live cell imaging data indicate that Mcl-1-inhibition induces apoptosis independent of mitosis in our breast cancer PDX, and activation of the direct mitochondrial apoptotic pathway [31] may outweigh the impact on cell cycle.

We also analyzed the impact of mitotic cyclin B stabilization by the PI bortezomib on the different taxane-sensitive solid cancers [30]. Both substances were sequentially used in low doses to obtain similar concentrations *in vitro* as achievable *in vivo* [2, 48]. It has been shown earlier that solid tumor cells can be as sensitive to PI as myeloma cells *in vitro* [49]. However, in clinical trials, bortezomib was neither effective in breast cancer alone or combined with doxorubicin, nor in chemotherapy-naive NSCLC [50], probably due to inhibition of only one of the three proteasomal subunits by the concentrations achieved *in vivo* [48]. We observed a synergistic effect of bortezomib with antimitotic treatment, but not by the assumed mitotic arrest with subsequent apoptosis: the apoptotic rate slightly increased after antimitotic treatment with PI, but cells entered apoptosis mainly during interphase or early mitosis, thus leading to a reduced mitotic rate, in particular in the breast cancer PDX. Mcl-1-expression is also regulated by proteasomal degradation, and its bortezomib-induced stabilization may inhibit apoptosis following antimitotic therapy [21]. However, it has been shown

that bortezomib converts Mcl-1 into a derivative with proapoptotic function [51]. We observed a highly toxic effect of low-dosed bortezomib in breast cancer, supporting the theory that bortezomib-induced stabilization of antiapoptotic Mcl-1 is overcome by this conversion into a proapoptotic form.

Taken together, the combination of antimitotic substances with APC/C-inhibitors or clinically approved PI seems a promising approach to improve treatment response in different solid tumors, even though they act via different entity-dependent mechanisms; in case of high Mcl-1-expression encouraging results could be obtained by additional application of an appropriate Mcl-1-inhibitor. In light of our results, we propose that a strong antitumor effect can be obtained by the combination of low concentrations that are achievable *in vivo* and that help to reduce clinically relevant side effects and resistance development against single drugs. Our data emphasize the importance of a molecular characterization and risk stratification to identify patients that may not respond to standard antimitotic treatment and to allow an individual therapy planning.

Acknowledgements

The project was presented in part at annual meetings of the German Society for Hematology and Oncology (DGHO) and intra-departmental meetings. We thank the participants of these meetings for advice and very fruitful discussion, and the members of the Lighthouse Core Facility Freiburg for excellent technical assistance.

Disclosure of conflict of interest

None.

Address correspondence to: Ralph Wäsch, Department of Hematology, Oncology and Stem Cell Transplantation, Medical Center - University of Freiburg, Faculty of Medicine, University of Freiburg, Freiburg, Germany. E-mail: Ralph.Waesch@uniklinik-freiburg.de

References

[1] Dominguez-Brauer C, Thu KL, Mason JM, Blaser H, Bray MR and Mak TW. Targeting mitosis in cancer: emerging strategies. Mol Cell 2015; 60: 524-36.

[2] Weaver BA. How Taxol/paclitaxel kills cancer cells. Mol Biol Cell 2014; 25: 2677-81.

[3] Zasadil LM, Andersen KA, Yeum D, Rocque GB, Wilke LG, Tevaarwerk AJ, Raines RT, Burkhard ME and Weaver BA. Cytotoxicity of paclitaxel in breast cancer is due to chromosome missegregation on multipolar spindles. Sci Transl Med 2014; 6: 229ra43.

[4] Alves RC, Fernandes RP, Eloy JO, Salgado HRN and Chorilli M. Characteristics, properties and analytical methods of paclitaxel: a review. Crit Rev Anal Chem 2018; 48: 110-8.

[5] Stukenberg PT and Burke DJ. Connecting the microtubule attachment status of each kinetochore to cell cycle arrest through the spindle assembly checkpoint. Chromosoma 2015; 124: 463-80.

[6] Musacchio A and Salmon ED. The spindle-assembly checkpoint in space and time. Nat Rev Mol Cell Biol 2007; 8: 379-93.

[7] Wäsch R and Engelbert D. Anaphase-promoting complex-dependent proteolysis of cell cycle regulators and genomic instability of cancer cells. Oncogene 2005; 24: 1-10.

[8] Peters JM. The anaphase promoting complex/cyclosome: a machine designed to destroy. Nat Rev Mol Cell Biol 2006; 7: 644-56.

[9] Wäsch R and Cross FR. APC-dependent proteolysis of the mitotic cyclin Clb2 is essential for mitotic exit. Nature 2002; 418: 556-62.

[10] Schnerch D, Yalcintepe J, Schmidts A, Becker H, Follo M, Engelhardt M and Wäsch R. Cell cycle control in acute myeloid leukemia. Am J Cancer Res 2012; 2: 508-28.

[11] Schrock MS, Stromberg BR, Scarberry L and Summers MK. APC/C ubiquitin ligase: functions and mechanisms in tumorigenesis. Semin Cancer Biol 2020; 67: 80-91.

[12] Topham CH and Taylor SS. Mitosis and apoptosis: how is the balance set? Curr Opin Cell Biol 2013; 25: 780-5.

[13] Fujiwara T, Bandi M, Nitta M, Ivanova EV, Bronson RT and Pellman D. Cytokinesis failure generating tetraploids promotes tumorigenesis in p53-null cells. Nature 2005; 437: 1043-7.

[14] Gascoigne KE and Taylor SS. Cancer cells display profound intra- and interline variation following prolonged exposure to antimitotic drugs. Cancer Cell 2008; 14: 111-22.

[15] Brito DA and Rieder CL. Mitotic checkpoint slippage in humans occurs via cyclin B destruction in the presence of an active checkpoint. Curr Biol 2006; 16: 1194-200.

[16] Schnerch D, Follo M, Krohs J, Felthaus J, Engelhardt M and Wäsch R. Monitoring APC/C activity in the presence of chromosomal misalignment in unperturbed cell populations. Cell Cycle 2012; 11: 310-21.

[17] Schnerch D, Schüler J, Follo M, Felthaus J, Wider D, Klingner K, Greil C, Duyster J, Engel-

hardt M and Wäsch R. Proteasome inhibition enhances the efficacy of volasertib-induced mitotic arrest in AML in vitro and prolongs survival in vivo. Oncotarget 2017; 8: 21153-66.
[18] Delbridge AR, Grabow S, Strasser A and Vaux DL. Thirty years of BCL-2: translating cell death discoveries into novel cancer therapies. Nat Rev Cancer 2016; 16: 99-109.
[19] Akgul C. Mcl-1 is a potential therapeutic target in multiple types of cancer. Cell Mol Life Sci 2009; 66: 1326-36.
[20] Beroukhim R, Mermel CH, Porter D, Wei G, Raychaudhuri S, Donovan J, Barretina J, Boehm JS, Dobson J, Urashima M, Mc Henry KT, Pinchback RM, Ligon AH, Cho YJ, Haery L, Greulich H, Reich M, Winckler W, Lawrence MS, Weir BA, Tanaka KE, Chiang DY, Bass AJ, Loo A, Hoffman C, Prensner J, Liefeld T, Gao Q, Yecies D, Signoretti S, Maher E, Kaye FJ, Sasaki H, Tepper JE, Fletcher JA, Tabernero J, Baselga J, Tsao MS, Demichelis F, Rubin MA, Janne PA, Daly MJ, Nucera C, Levine RL, Ebert BL, Gabriel S, Rustgi AK, Antonescu CR, Ladanyi M, Letai A, Garraway LA, Loda M, Beer DG, True LD, Okamoto A, Pomeroy SL, Singer S, Golub TR, Lander ES, Getz G, Sellers WR and Meyerson M. The landscape of somatic copy-number alteration across human cancers. Nature 2010; 463: 899-905.
[21] Harley ME, Allan LA, Sanderson HS and Clarke PR. Phosphorylation of Mcl-1 by CDK1-cyclin B1 initiates its Cdc20-dependent destruction during mitotic arrest. EMBO J 2010; 29: 2407-20.
[22] Sackton KL, Dimova N, Zeng X, Tian W, Zhang M, Sackton TB, Meaders J, Pfaff KL, Sigoillot F, Yu H, Luo X and King RW. Synergistic blockade of mitotic exit by two chemical inhibitors of the APC/C. Nature 2014; 514: 646-9.
[23] Raab M, Sanhaji M, Zhou S, Rödel F, El-Balat A, Becker S and Strebhardt K. Blocking mitotic exit of ovarian cancer cells by pharmaceutical inhibition of the anaphase-promoting complex reduces chromosomal instability. Neoplasia 2019; 21: 363-75.
[24] Raab M, Kobayashi NF, Becker S, Kurunci-Csacsko E, Krämer A, Strebhardt K and Sanhaji M. Boosting the apoptotic response of high-grade serous ovarian cancers with CCNE1 amplification to paclitaxel in vitro by targeting APC/C and the pro-survival protein MCL-1. Int J Cancer 2020; 146: 1086-98.
[25] Sinnott R, Winters L, Larson B, Mytsa D, Taus P, Cappell KM and Whitehurst AW. Mechanisms promoting escape from mitotic stress-induced tumor cell death. Cancer Res 2014; 74: 3857-69.
[26] Giovinazzi S, Bellapu D, Morozov VM and Ishov AM. Targeting mitotic exit with hyperthermia or APC/C inhibition to increase paclitaxel efficacy. Cell Cycle 2013; 12: 2598-607.
[27] Leverson JD, Zhang H, Chen J, Tahir SK, Phillips DC, Xue J, Nimmer P, Jin S, Smith M, Xiao Y, Kovar P, Tanaka A, Bruncko M, Sheppard GS, Wang L, Gierke S, Kategaya L, Anderson DJ, Wong C, Eastham-Anderson J, Ludlam MJ, Sampath D, Fairbrother WJ, Wertz I, Rosenberg SH, Tse C, Elmore SW and Souers AJ. Potent and selective small-molecule MCL-1 inhibitors demonstrate on-target cancer cell killing activity as single agents and in combination with ABT-263 (navitoclax). Cell Death Dis 2015; 6: e1590.
[28] Wäsch R. Targeting mitotic exit for cancer treatment. Expert Opin Ther Targets 2011; 15: 785-8.
[29] Jordan MA and Wilson L. Microtubules as a target for anticancer drugs. Nat Rev Cancer 2004; 4: 253-65.
[30] Smolders L and Teodoro JG. Targeting the anaphase promoting complex: common pathways for viral infection and cancer therapy. Expert Opin Ther Targets 2011; 15: 767-80.
[31] Kotschy A, Szlavik Z, Murray J, Davidson J, Maragno AL, Le Toumelin-Braizat G, Chanrion M, Kelly GL, Gong JN, Moujalled DM, Bruno A, Csekei M, Paczal A, Szabo ZB, Sipos S, Radics G, Proszenyak A, Balint B, Ondi L, Blasko G, Robertson A, Surgenor A, Dokurno P, Chen I, Matassova N, Smith J, Pedder C, Graham C, Studeny A, Lysiak-Auvity G, Girard AM, Gravé F, Segal D, Riffkin CD, Pomilio G, Galbraith LC, Aubrey BJ, Brennan MS, Herold MJ, Chang C, Guasconi G, Cauquil N, Melchiore F, Guigal-Stephan N, Lockhart B, Colland F, Hickman JA, Roberts AW, Huang DC, Wei AH, Strasser A, Lessene G and Geneste O. The MCL1 inhibitor S63845 is tolerable and effective in diverse cancer models. Nature 2016; 538: 477-82.
[32] EC50 Calculator|AAT Bioquest n.d. https://www.aatbio.com/tools/ec50-calculator.
[33] Chou TC. Theoretical basis, experimental design, and computerized simulation of synergism and antagonism in drug combination studies. Pharmacol Rev 2006; 58: 621-81.
[34] Engelbert D, Schnerch D, Baumgarten A and Wäsch R. The ubiquitin ligase APC Cdh1 is required to maintain genome integrity in primary human cells. Oncogene 2008; 27: 907-17.
[35] Conway T, Wazny J, Bromage A, Tymms M, Sooraj D, Williams ED and Beresford-Smith B. Xenome-a tool for classifying reads from xenograft samples. Bioinformatics 2012; 28: i172-8.
[36] McLaren W, Gil L, Hunt SE, Riat HS, Ritchie GR, Thormann A, Flicek P and Cunningham F. The ensembl variant effect predictor. Genome Biol 2016; 17: 122.

[37] Sherry ST, Ward MH, Kholodov M, Baker J, Phan L, Smigielski EM and Sirotkin K. dbSNP: the NCBI database of genetic variation. Nucleic Acids Res 2001; 29: 308-11.
[38] Lai Y, Wei X, Lin S, Qin L, Cheng L and Li P. Current status and perspectives of patient-derived xenograft models in cancer research. J Hematol Oncol 2017; 10: 106.
[39] Tentler JJ, Tan AC, Weekes CD, Jimeno A, Leong S, Pitts TM, Arcaroli JJ, Messersmith WA and Eckhardt SG. Patient-derived tumour xenografts as models for oncology drug development. Nat Rev Clin Oncol 2012; 9: 338-50.
[40] Zeng X, Sigoillot F, Gaur S, Choi S, Pfaff KL, Oh DC, Hathaway N, Dimova N, Cuny GD and King RW. Pharmacologic inhibition of the anaphase-promoting complex induces a spindle checkpoint-dependent mitotic arrest in the absence of spindle damage. Cancer Cell 2010; 18: 382-95.
[41] Goodwin CM, Rossanese OW, Olejniczak ET and Fesik SW. Myeloid cell leukemia-1 is an important apoptotic survival factor in triple-negative breast cancer. Cell Death Differ 2015; 22: 2098-106.
[42] Huang HC, Shi J, Orth JD and Mitchison TJ. Evidence that mitotic exit is a better cancer therapeutic target than spindle assembly. Cancer Cell 2009; 16: 347-58.
[43] Zeng X, Xu WK, Lok TM, Ma HT and Poon RYC. Imbalance of the spindle-assembly checkpoint promotes spindle poison-mediated cytotoxicity with distinct kinetics. Cell Death Dis 2019; 10: 1-15.
[44] Karra H, Repo H, Ahonen I, Löyttyniemi E, Pitkänen R, Lintunen M, Kuopio T, Söderström M and Kronqvist P. Cdc20 and securin overexpression predict short-term breast cancer survival. Br J Cancer 2014; 110: 2905-13.
[45] Kato T, Daigo Y, Aragaki M, Ishikawa K, Sato M and Kaji M. Overexpression of CDC20 predicts poor prognosis in primary non-small cell lung cancer patients. J Surg Oncol 2012; 106: 423-30.
[46] Campbell KJ, Dhayade S, Ferrari N, Sims AH, Johnson E, Mason SM, Dickson A, Ryan KM, Kalna G, Edwards J, Tait SWG and Blyth K. MCL-1 is a prognostic indicator and drug target in breast cancer. Cell Death Dis 2018; 9: 19.
[47] Wertz IE, Kusam S, Lam C, Okamoto T, Sandoval W, Anderson DJ, Helgason E, Ernst JA, Eby M, Liu J, Belmont LD, Kaminker JS, O'Rourke KM, Pujara K, Kohli PB, Johnson AR, Chiu ML, Lill JR, Jackson PK, Fairbrother WJ, Seshagiri S, Ludlam MJ, Leong KG, Dueber EC, Maecker H, Huang DC and Dixit VM. Sensitivity to antitubulin chemotherapeutics is regulated by MCL1 and FBW7. Nature 2011; 471: 110-4.
[48] Weyburne ES, Wilkins OM, Sha Z, Williams DA, Pletnev AA, de Bruin G, Overkleeft HS, Goldberg AL, Cole MD and Kisselev AF. Inhibition of the proteasome β2 site sensitizes triple-negative breast cancer cells to β5 inhibitors and suppresses Nrf1 activation. Cell Chem Biol 2017; 24: 218-30.
[49] Garnett MJ, Edelman EJ, Heidorn SJ, Greenman CD, Dastur A, Lau KW, Greninger P, Thompson IR, Luo X, Soares J, Liu Q, Iorio F, Surdez D, Chen L, Milano RJ, Bignell GR, Tam AT, Davies H, Stevenson JA, Barthorpe S, Lutz SR, Kogera F, Lawrence K, McLaren-Douglas A, Mitropoulos X, Mironenko T, Thi H, Richardson L, Zhou W, Jewitt F, Zhang T, O'Brien P, Boisvert JL, Price S, Hur W, Yang W, Deng X, Butler A, Choi HG, Chang JW, Baselga J, Stamenkovic I, Engelman JA, Sharma SV, Delattre O, Saez-Rodriguez J, Gray NS, Settleman J, Futreal PA, Haber DA, Stratton MR, Ramaswamy S, McDermott U and Benes CH. Systematic identification of genomic markers of drug sensitivity in cancer cells. Nature 2012; 483: 570-5.
[50] Dou QP and Zonder JA. Overview of proteasome inhibitor-based anti-cancer therapies: perspective on bortezomib and second generation proteasome inhibitors versus future generation inhibitors of ubiquitin-proteasome system. Curr Cancer Drug Targets 2014; 14: 517-36.
[51] Podar K, Gouill SL, Zhang J, Opferman JT, Zorn E, Tai YT, Hideshima T, Amiot M, Chauhan D, Harousseau JL and Anderson KC. A pivotal role for Mcl-1 in Bortezomib-induced apoptosis. Oncogene 2008; 27: 721-31.

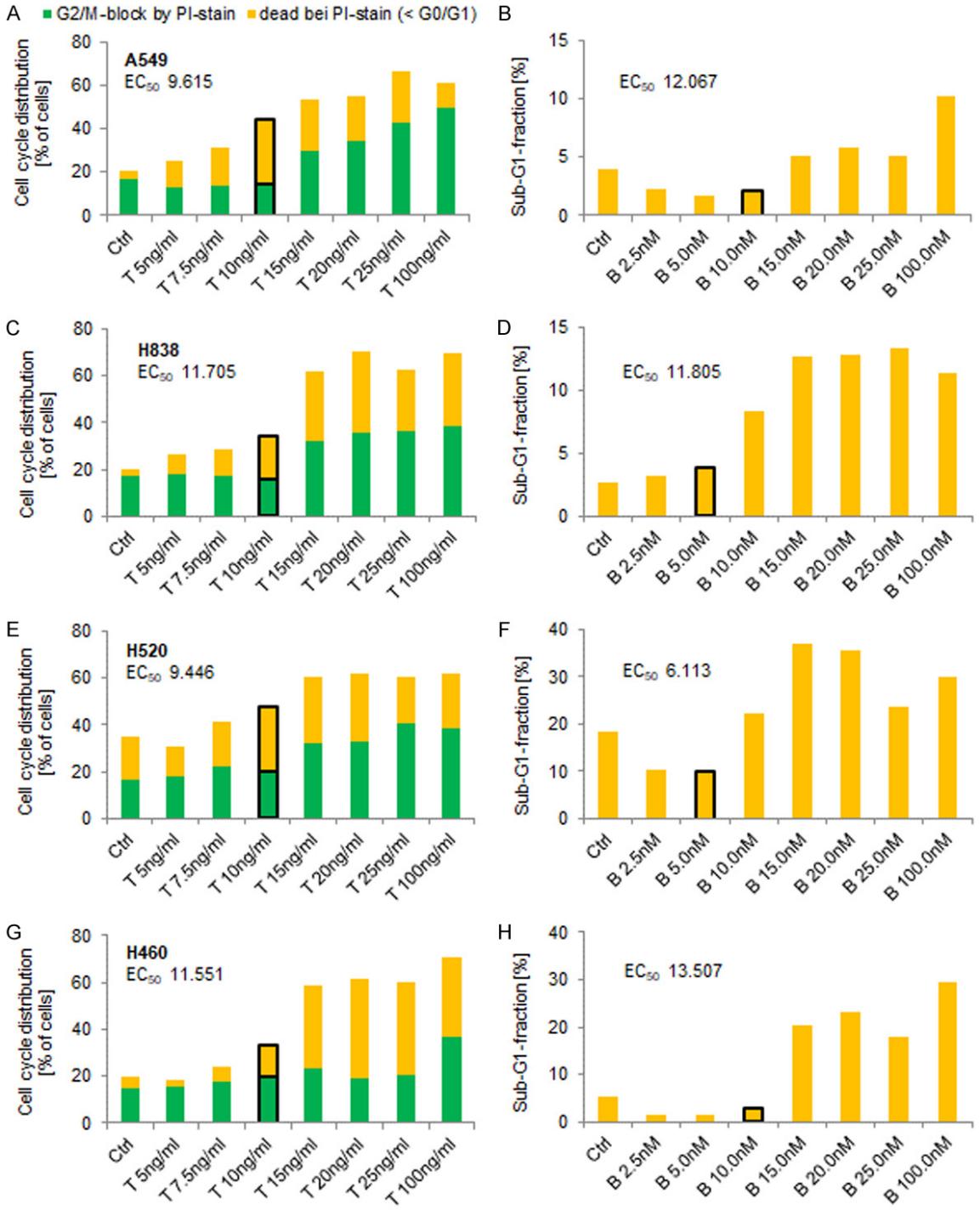

Figure S1. Concentration series to determine the lowest dose of paclitaxel leading to an increased G2/M-arrest and the lowest dose of bortezomib leading to an increased apoptotic rate in NSCLC cell lines. NSCLC adenocarcinoma [A549 and H838], squamous [H520] and large cell carcinoma [H460] cell lines were treated with rising concentrations of (A, C, E, G) the spindle poison paclitaxel and (B, D, F, H) the proteasome inhibitor bortezomib and assessed by flow cytometry after propidium iodide-stain, the percentage of cells in G2/M-phase (green bars) and apoptotic cells (yellow bars) is depicted as compared to control. The dose chosen for further experiments is marked with a black box. Abbreviations: NSCLC = Non-small cell lung cancer; ctrl = untreated control; T = paclitaxel; B = bortezomib; EC_{50} = half maximal effective concentration.

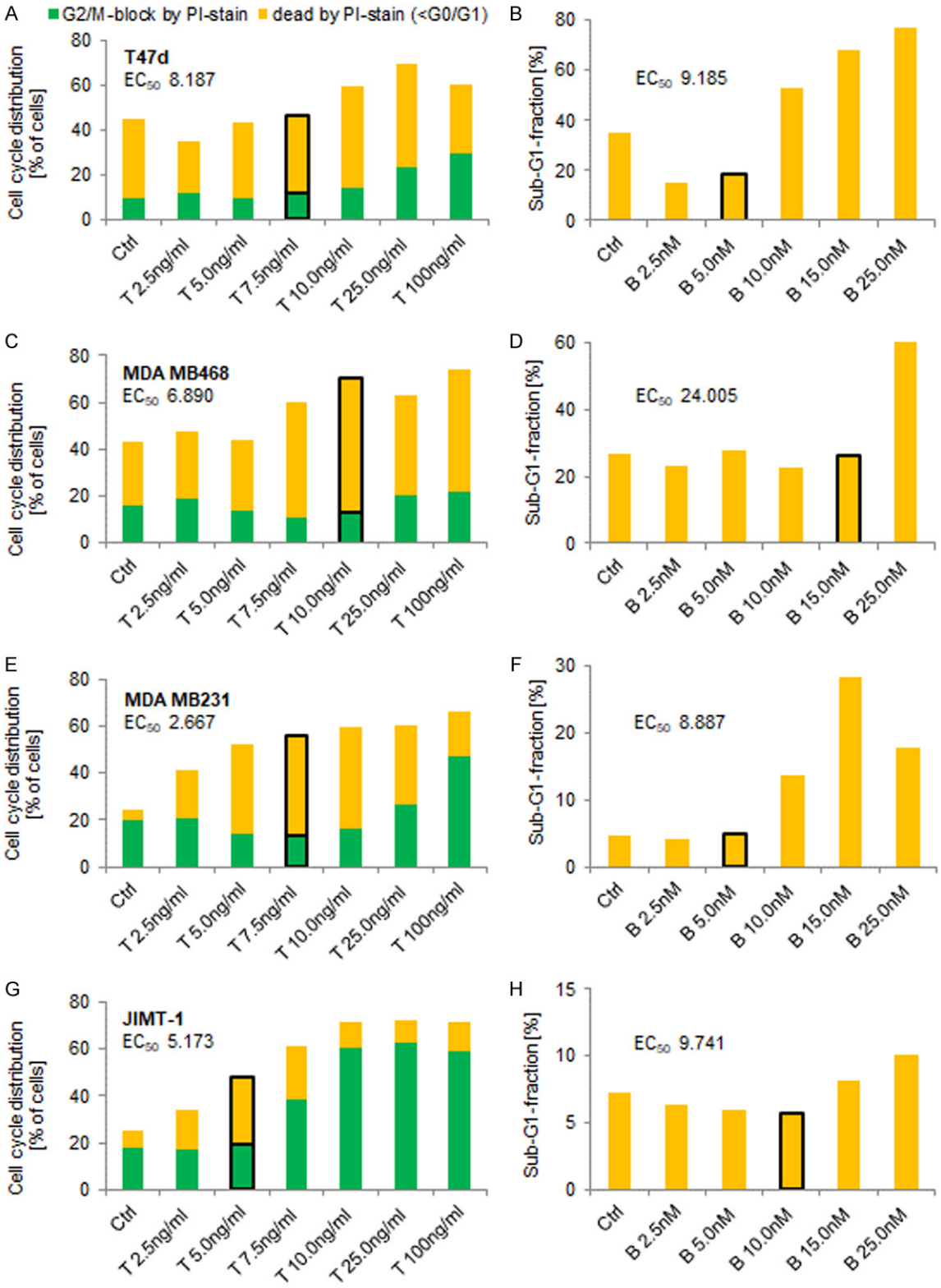

Figure S2. Concentration series to determine the lowest dose of paclitaxel leading to an increased G2/M-arrest and the lowest dose of bortezomib leading to an increased apoptotic rate in breast cancer cell lines. Breast cancer cell lines (hormone receptor-positive [T47D] and triple negative [MDA MB468, MDA MB231, JIMT-1]) were treated with (A, C, E, G) the spindle poison paclitaxel and (B, D, F, H) the proteasome inhibitor bortezomib and assessed by flow cytometry after propidium iodide-stain, the percentage of cells in G2/M-phase (green bars) and apoptotic cells (yellow bars) is depicted as compared to control. The dose chosen for further experiments is marked with a black box. Abbreviations: ctrl = untreated control; T = paclitaxel; B = bortezomib; EC_{50} = half maximal effective concentration.

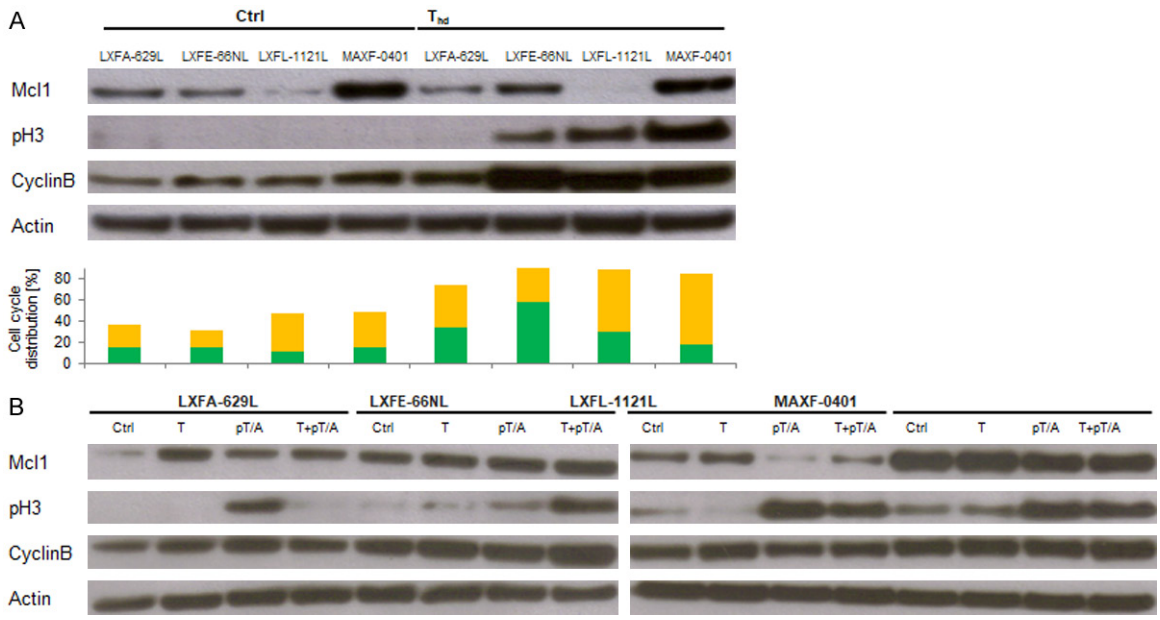

Figure S3. Cell cycle dependent Mcl-1-levels. Mcl-1-expression was analyzed by western blot of NSCLC squamous cell carcinoma [LXFE-66NL], adenocarcinoma [LXFA-629L], large cell carcinoma [LXFL-1121L] and breast cancer PDX [MAXF-0401] in (A) untreated cells and after G2/M-block with high-dosed paclitaxel (T_{hd}) and (B) after treatment with low-dosed paclitaxel (T), APC/C-inhibition (pT/A) and the combination (T + pT/A). The percentage of cells in G2/M-phase (green bars) and apoptotic cells (yellow bars) was assessed by flow cytometry after propidium iodide-stain in parallel experiments, the appropriate diagrams for (B) are depicted in **Figure 4C**. Abbreviations: NSCLC = Non-small cell lung cancer; PDX = patient-derived xenograft; ctrl = untreated control; T_{hd} = high-dosed paclitaxel; pH3 = phospho-Histone 3; T = low-dosed paclitaxel; pT/A = proTAME/apcin.